Mater. Res. Soc. Symp. Proc. Vol. 1202 © 2010 Materials Research Society 1202-I5.21-1

Growth temperature - phase stability relation in $In_{1-x}Ga_xN$ epilayers grown by high-pressure CVD

G. Durkaya[1], M. Alevli[1], M. Buegler[1,2], R. Atalay[1], S. Gamage[1], M. Kaiser[2], R. Kirste[2], A. Hoffmann[2], M. Jamil[3], I. Ferguson[3] and N. Dietz[1]
[1] Department of Physics & Astronomy, Georgia State University, Atlanta, GA 30303
[2] Technical University Berlin, Institute of Solid State Physics, Berlin, Germany
[3] School of ECE, University of North Carolina at Charlotte, Charlotte, NC 28223

ABSTRACT

The influence of the growth temperature on the phase stability and composition of single-phase $In_{1-x}Ga_xN$ epilayers has been studied. The $In_{1-x}Ga_xN$ epilayers were grown by high-pressure Chemical Vapor Deposition with nominally composition of x = 0.6 at a reactor pressure of 15 bar at various growth temperatures. The layers were analyzed by x-ray diffraction, optical transmission spectroscopy, atomic force microscopy, and Raman spectroscopy. The results showed that a growth temperature of 925 °C led to the best single phase InGaN layers with the smoothest surface and smallest grain areas.

INTRODUCTION

The ternary $In_{1-x}Ga_xN$ alloy system attracts significant attention due to its unique physical properties such as direct band-gap, high carrier mobility, and strong chemical bonding[1,2]. The optical band gap of the $In_{1-x}Ga_xN$ alloy system can be tuned from ultraviolet (E_g^{GaN}=3.4 eV) to near-infrared (E_g^{InN}=0.7eV), spanning over more than 80% of the solar spectrum. This is of interest for the development of high-efficiency monolithic multijunction photovoltaic solar cells based on $In_{1-x}Ga_xN$ / $Ga_{1-x}In_xN$ heterostructures. However, the growth of the $In_{1-x}Ga_xN$ alloys and heterostructures is a challenge due to the lower disassociation temperature of InN compared to that of GaN. A further challenge is the large difference between the lattice constants of the binaries InN and GaN[3] (~11%), which may induce lattice strain[4] and contribute to a potential solid-phase miscibility gap in the ternary $In_{1-x}Ga_xN$ system[5]. These facts contribute to the reported compositional inhomogeneity observed in InGaN layers[6-11], which reduces the device efficiencies of InGaN based optoelectronic structures.

The phase stability of InGaN epilayers has been studied for different growth temperatures with different growth techniques[7,10,11]. For instance, InGaN layers grown by RF-MBE show a linear correlation between gallium incorporationwith increased growth temperature between 600°C - 700°C[10]. MOVPE grown InGaN layers exhibited a similar behavior in the temperature range between 700°C - 850°C[12]. Pantha et al.[7] reported the growth of single phase InGaN layers by MOCVD and observed a decreased indium incorporation with increasing growth temperature from 600°C - 750°C. This research effort explores the potential of high-pressure Chemical Vapor Deposition (HPCVD) to improve the phase stability in InGaN layers, utilizing high pressures nitrogen gas to stabilize the $In_{1-x}Ga_xN$ growth surface and effectively suppressing the thermal decomposition process above the growth surface[12,13]. This contribution focuses on the characterization of a set of single-phase $In_{1-x}Ga_xN$ layers that were

grown under identical growth conditions, varying the growth temperature only. X-Ray Diffraction (XRD), Optical Transmission Spectroscopy (OTS), and Raman spectroscopy were used to analyze the structural and optical properties of the epilayers. The findings were linked to the surface morphological properties of the $In_{1-x}Ga_xN$ layers.

EXPERIMENTAL DETAILS

The $In_{1-x}Ga_xN$ epilayers analyzed were grown by HPCVD on ~5 μm thick GaN/c-plane sapphire templates. Trimethylindium (TMI), Trimethylgallium (TMG) and ammonia (NH_3) precursors were used to provide active indium, gallium and nitrogen fragments respectively to the growth surface. As depicted in Figure 1, the precursors were provided to the growth surface via temporally controlled precursor pulses, which are embedded into the nitrogen main carrier gas stream. NH_3 and (TMI, TMG) injection times were 2.0 sec and 0.8 sec, respectively. The pulse separations between TMI/TMG - ammonia and between ammonia - TMI/TMG were set to 1.4 sec and 2.2 sec, respectively. The $In_{1-x}Ga_xN$ layers were grown at a reactor pressure of 15 bar, a nitrogen (N_2) main carrier gas flow of 12 slm (standard liters per minute), a group V-III molar precursor ratio of 1500, and a group III composition set value of x = 0.6. All experimental parameters were kept constant except the growth temperature, which was varied between 910°C and 960°C.

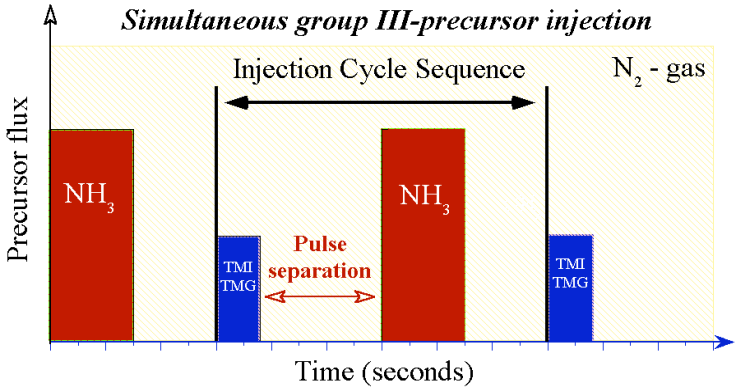

Figure 1.

The pulsed injection sequence employed for $In_{1-x}Ga_xN$ growth

XRD experiments were carried out utilizing an X`Pert PRO MPD (Philips) 4-circle diffractometer with a monochromatic X-ray (CuKα) source. XRD spectra were analyzed by Gaussian curve fitting to determine the position and Full Width Half Maximum (FWHM) of the (0002) Bragg reflex. The position and corresponding miller indices of this Bragg reflex were evaluated together to calculate the lattice parameter *'c'* of the $In_{1-x}Ga_xN$ layers[3]. The composition of the $In_{1-x}Ga_xN$ epilayers were estimated using Vegard's law, which assumes a linear dependence of the ternary lattice parameters and their binaries alloys GaN and InN, respectively. Neglecting further any interfacial strain effects on XRD spectra, the lattice parameter 'c' can be expressed as

$$c_o^{In_{1-x}Ga_xN} = x \cdot c_o^{GaN} + (1-x) \cdot c_o^{InN} \qquad (1)$$

In order to analyze the behavior of the absorption edge of $In_{1-x}Ga_xN$ layers for different growth temperatures, optical transmission experiments were carried out at room temperature using a UV-VIS-NIR spectrometer. The acquired optical transmission spectra were corrected for detector, monochromator and light source characteristics and normalized to the growth templates

used. The optical absorption spectra (OAS) of the layers were calculated from the optical transmission spectra using Beer–Lambert's law in order to estimate the optical absorption edge of the $In_{1-x}Ga_xN$ alloys. The surface morphology of the layers was analyzed by Atomic Force Microscopy (AFM) using a 'XE 100 Park Systems' AFM in non-contact mode. The AFM tips used in the AFM experiments had a resonance frequency of 300 kHz and a spring constant of 45N/m. The phonon modes of the $In_{1-x}Ga_xN$ layers were studied by Raman spectroscopy in back-scattering geometry (z(xx)$\underline{z}$) using an excitation wavelength of 532nm. The Raman spectra were analyzed using a Lorentzian peak fitting algorithm in order to obtain peak positions and FWHM's values for the phonon modes.

RESULTS AND DISCUSSION

Figure 2a shows 2Θ-ω scans for the $In_{1-x}Ga_xN$ layers with a nominally composition value x=0.60 grown at growth temperatures ranging from 910°C to 960°C. All epilayers exhibit single $In_{1-x}Ga_xN$ (0002) Bragg reflexes, indicating no macroscopic observable phase separations. The line-shapes and peak positions of the $In_{1-x}Ga_xN$ (0002) Bragg reflexes show a strong dependency with growth temperature. The line-shape and peak position analysis of these Bragg reflexes are summarized in Table 1. The $In_{1-x}Ga_xN$ layer grown at 925°C exhibited the most pronounced $In_{1-x}Ga_xN$ (0002) Bragg reflex. The estimated InGaN composition as a function of growth temperature is depicted in Figure 2b. The red dashed line in Figure 2b marks the experimental set-point, defined by the set values for the precursors TMI and TMG in the gas phase. Figure 2b indicates a nonlinear correlation between the molar group III-ratio in the gas phase and bulk layer, with a closest match for 925°C for which the highest indium incorporation is observed.

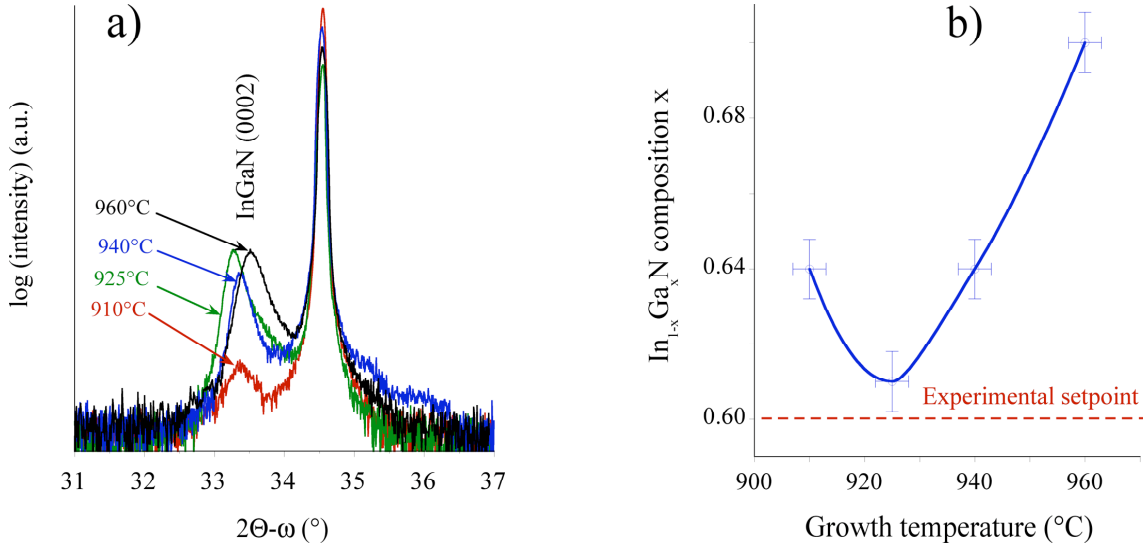

Figure 2. a) XRD patterns and **b)** estimated composition for $In_{1-x}Ga_xN$ epilayers grown on GaN/c-sapphire templates with different growth temperatures varying from 910°C to 960°C

The optical absorption spectra obtained for the $In_{1-x}Ga_xN$ epilayers grown at different temperatures are shown in Figure 3a. As shown, the optical absorption edge changes as a function of the growth temperature. To quantify the absorption edge, a linear slope fit of the curves was used to obtain the intercept point with the energy axis. The calculated intercept values are plotted in Figure 3b as a function of the growth temperature. The estimate shows that

the absorption-edge follows the indium composition behavior shown in Figure 2b. The highest indium incorporation is observed for a growth temperature of 925°C with decreasing indium content as the growth temperature increases to 960°C.

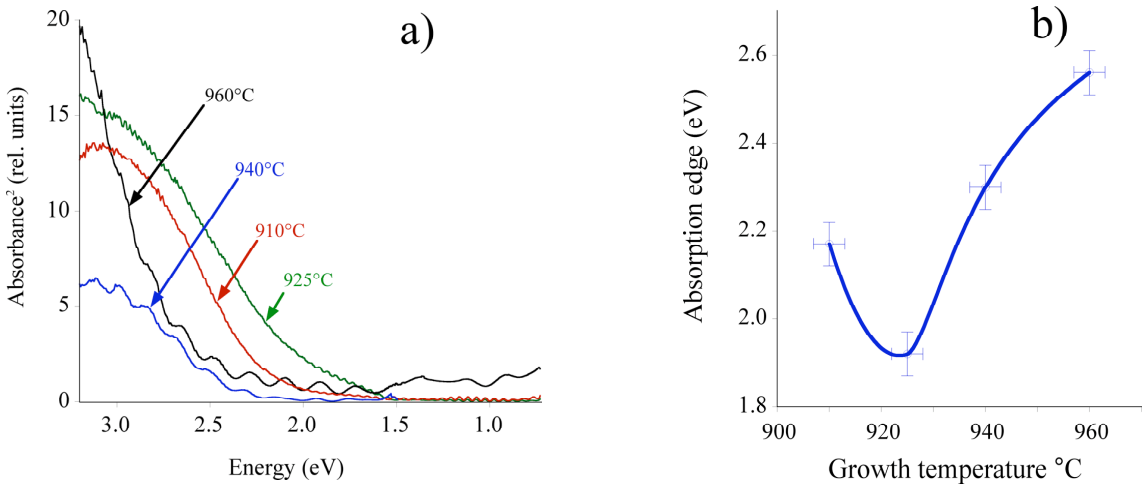

Figure 3. a) OAS spectra and **b)** calculated absorption edge of $In_{1-x}Ga_xN$ layers grown at different growth temperatures from 910 °C to 960 °C

Figure 4.a, b, c and, d depict 2μm x 2μm AFM images of the $In_{1-x}Ga_xN$ epilayers grown at 910°C, 925°C, 940°C, and 960°C, respectively. Statistical analysis techniques were used to calculate the surface roughnesses and average grain areas of these AFM images. The correlation of surface roughness and average grain area as function of growth temperature are shown in the Figure 4e. With increasing growth temperature from 910°C to 925° the surface roughness and average grain area decrease and than increase as the growth temperature increases to 960°C.

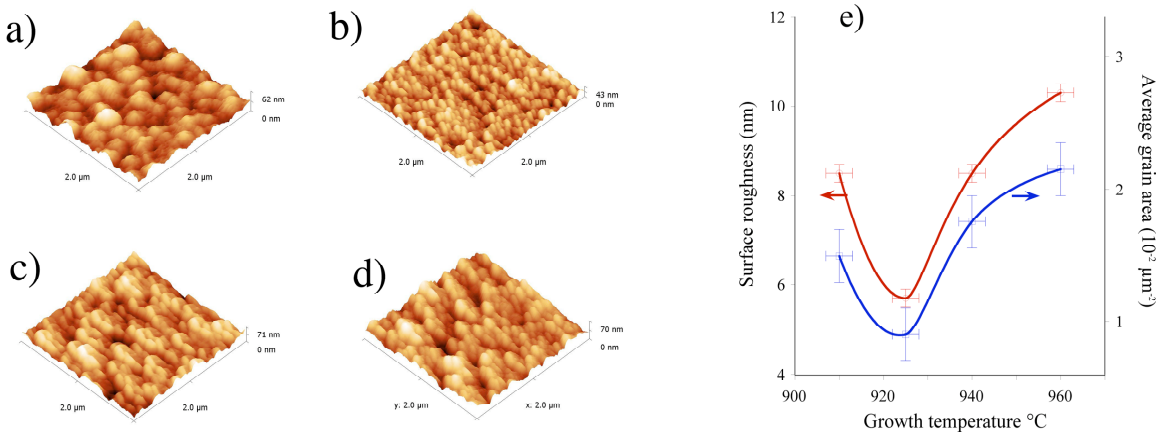

Figure 4. (a-d) 2μm x 2μm AFM images of $In_{1-x}Ga_xN$ layers grown at **a)** 910°C, **b)** 925°C, **c)** 940°C, **d)** 960°C , **e)** Surface roughness and average grain area as a function of the growth temperature.

The Raman spectra for the $In_{1-x}Ga_xN$ epilayers are shown in Figure 5a in the frequency region for the E_2(high) and A_1(LO) phonon modes. In wurtzite InN and GaN, the Raman phonon modes allowed in z(xx)$\underline{z}$ geometry along (0001) direction are A_1(LO) and E_2(high[14]. The most distinct phonon mode observed in the Raman spectra is the A_1(LO) mode, while the E_2(high) mode is present, but not distinct enough to be statistically analyzed. The A_1(LO) Raman line was fitted using two Lorentzian oscillators side by side. The curve fitting results are summarized in

Table 1 and variations in the peak positions as a function of growth temperature is depicted in Figure 5b. The two oscillator contribution are denoted as low - and high energy A_1(LO) oscillator, respectively. Also drawn in is the $In_{1-x}Ga_xN$ A_1(LO) mode position as function of composition x, assuming a linear behavior of the A_1(LO) mode between the binaries. The fitted high energy A_1(LO) oscillator peak corresponds to the major phase according to the peak area analysis as shown in Table 1 and its position follows very closely a single A_1(LO) mode behavior. The origin and behavior of low energy A_1(LO) oscillator will need further studies.

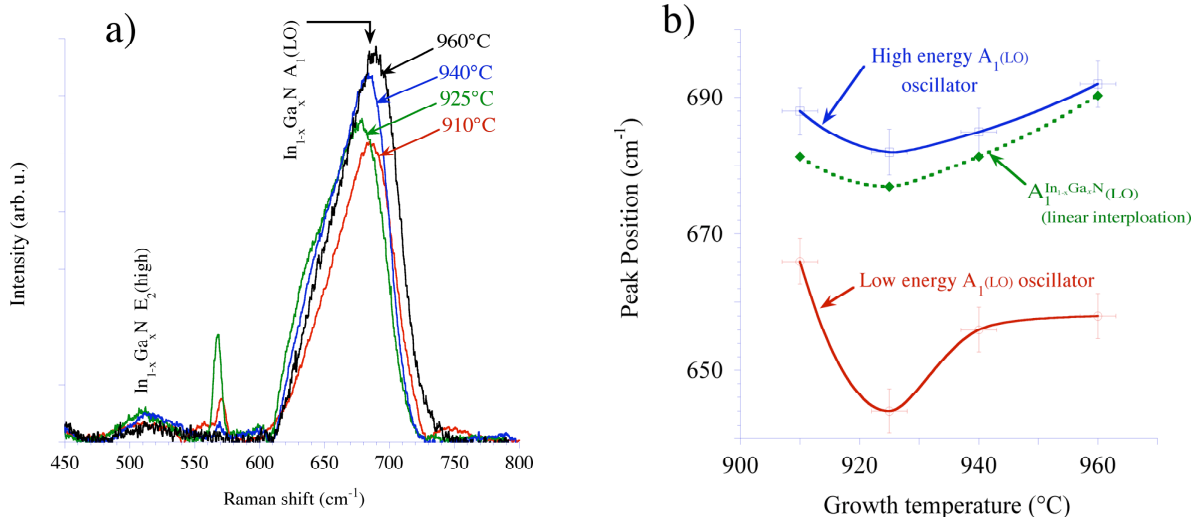

Figure 5. a) Raman spectra of E_2(high) and A_1(LO) region for $In_{1-x}Ga_xN$ layers grown with different growth temperatures, b) A_1(LO) phonon peak positions for the $In_{1-x}Ga_xN$ epilayers.

	Growth temperature	910°C	925°C	940°C	960°C
XRD (0002)	2-θ (in deg)	33.36	33.31	33.38	33.56
	FWHM (arcsec)	2160	1210	1510	2110
	Estimated composition x	0.64	0.61	0.64	0.70
OAS	Absorption edge (eV)	2.2	1.9	2.3	2.6
AFM	Surface roughness (nm)	8.5	5.7	8.6	10.3
	Ave. grain area (10^{-2} μm^2)	1.5	0.9	1.8	2.2
RAMAN	Low energy side position (cm^{-1})	666	644	656	658
	Low energy side FWHM (cm^{-1})	60	43	49	47
	High energy side position (cm^{-1})	688	682	685	693
	High energy side FWHM (cm^{-1})	33	38	32	34
	Area ratio (High energy peak / Low energy peak)	1.5	1.6	1.5	1.8

Table 1. Summary of the results obtained from XRD, AFM, OAS, and Raman spectroscopy analyzing $In_{1-x}Ga_xN$ layers with a nominal set value of x = 0.6, as a function of growth temperature.

The XRD analysis suggests that – under the set of chosen growth conditions - at the growth temperature of 925°C the highest amount of indium was incorporated in the $In_{1-x}Ga_xN$ (x=0.61) epilayers. Smaller and high growth temperatures led the less indium incorporation and reduced structural quality. The XRD (0002) Bragg reflex from the $In_{1-x}Ga_xN$ layer grown at 925°C showed an optimum, but is at least a factor 3 to 5 too high for device quality material. The same $In_{1-x}Ga_xN$ layer, showed the lowest optical absorption edge, the smoothest surface roughness and

the smallest average grain area. The A_1(LO) phonon line in Raman spectra had to be fitted using two contributions, where the high energy oscillator position follows closely a single A_1(LO) mode behavior with composition x. The low energy oscillator in the A_1(LO) peak might be due to microscopic compositional fluctuations that are not observable in XRD spectra, however, a further analysis is required to understand the origin and behavior of low energy contribution to the A_1(LO) mode peak. The results from Raman analysis are in good agreement with those reported by Hernandez et al.,[15] in which the higher indium incorporation shifted the LO phonons to lower energies, while the spectral line-shape is broadened. Although the growth temperature 925°C exhibits the highest phase stability, further studies in intermediate steps of the investigated growth temperatures are needed in order to realize the peculiarity of this growth temperature.

CONCLUSIONS

We have studied the compositional variations in single-phase $In_{1-x}Ga_xN$ (x=0.6) epilayers grown by HPCVD in the temperature range of 910°C - 960°C. XRD analysis revealed single phase epilayers with a local structural optimum at growth temperature of 925°C, which coincide with the smoothest surface morphology and the smallest average grain area as analyzed by AFM analysis. The line shape analysis of the A_1(LO) phonon mode observed in Raman spectroscopy indicates the highest strain component for a growth temperature of 925°C, at which the indium incorporation was closest to the set molor group III ratio in the gas phase.

ACKNOWLEDGMENTS

We gratefully acknowledge the support by AFOSR grant# FA9550-07-1-0345 and GSU-REP.

REFERENCES

1. H. Morkoc, *Nitride semiconductors and devices*, Springer-Verlag, (1999).
2. Wu, J., W. Walukiewicz, K. M. Yu, W. Shan, J. W. Ager III, E. E. Haller, H. Lu and W. J. Schaff, W. K. Metzger, S. Kurtz, J. of Appl. Phys. 94(10): 6477 6482. (2003).
3. F.K. Yam, Z. Hassan, Superlatt. and Microstr., 43 1–23 (2008).
4. S. Yu. Karpov, MRS Internet J. Nitride Semicond. Res. 3, 16 (1998).
5. I. Ho, G.B. Stringfellow, Appl. Phys. Lett. 69, 2701-2703 (1996).
6. R. Singh, D. Doppalapudi, T. D. Moustakas, and L. T. Romano, Appl. Phys. Lett. 70, 1089 (1997)
7. B. N. Pantha, J. Li, J. Y. Lin, and H. X. Jiang, Appl. Phys. Lett. 93, 182107 (2008)
8. N. A. El-Masry, E. L. Piner, S. X. Liu, and S. M. Bedair, Appl. Phys. Lett. 72, 40 (1998).
9. C.A. Chang, C. F. Shin, N. C. Chen, T. Y. Lin, and K. S. Liu, Appl. Phys. Lett. 85, 6131, (2004)
10. K. Kushi, H. Sasamoto, D. Sugihara, S. Nakamura, A. Kikuchi and K. Kishino, Mater. Sci. Eng. B, 59 (1999).
11. W. Van der Stricht, I. Moerman, P. Demeester, L. Considine, E.J. Thrush and J.A. Crawley, MRS Internet J. Nitride Semicond. Res. 2 (1997).
12. N. Dietz, in "*III-Nitrides Semiconductor Materials*", Ed. Z.C. Feng, Imperial College Press, ISBN 1-86094-636-4, pp. 203-235 (2006).
13. J. McChesney, P. M. Bridenbaugh, and P. B. O'Connor, Mater. Res. Bull. 5, 783 (1970).
14. V. Y. Davydov and A. A. Klochikhin, Semiconductors 38**,** 861-898 (2004).
15. S. Hernández, R. Cuscó, D. Pastor, L. Artús, K. P. O'Donnell, R. W. Martin, I. M. Watson, Y. Nanishi, and E. Calleja. J. of Appl. Phys. 97 013511 (2005)